Regulation of fish stocks without stock-recruitment relationships: the case of small pelagic fish

April 27, 2020

Running title: Regulation of anchovy populations

T. Mariella Canales: Center of Applied Ecology and Sustainability (CAPES), Pontificia Universidad Católica de Chile, Av. Alameda 340, Santiago, Chile

mariella.canales@gmail.com

Gustav W. Delius: Department of Mathematics, University of York, Heslington, York YO10 5DD, UK.

gustav.delius@york.ac.uk

Richard Law: York Cross-Disciplinary Centre for Systems Analysis, Ron Cooke Hub, University of York, York YO10 5GE, UK.

richard.law@york.ac.uk

Corresponding author Email: mariella.canales@gmail.com

Abstract

Small pelagic fish lack clear stock-recruitment relationships. This is a problem because such relationships are taken to be the primary descriptors of density dependence, responsible for regulating population density. In this paper, we show that a small pelagic fish species, anchovy, living in a stochastic environment, can be strongly regulated without a stock-recruitment relationship emerging. This is done through numerical analysis of a size-spectrum model, in which fish grow by eating and die in part from being eaten, with the result that birth, growth and death are all density dependent. The model includes cannibalism, and growth-dependent larval mortality, both of which have been suggested as regulatory mechanisms in anchovy, together with growth and reproduction later in life. Despite the lack of a clear stock-recruitment relationship in the presence of stochasticity, signals of density dependence in the vital rates remain clear, suggesting that they might prove to be better indicators of density dependence than stock-recruitment relationships in small pelagic fish.

KEYWORDS
anchovy, density dependence, growth, plankton, size-spectrum, stochasticity.

Contents

1 INTRODUCTION **4**

2 METHODS **6**

2.1 Fish population dynamics 6

2.2 Plankton dynamics 9

2.3 Numerical methods 10

3 RESULTS **11**

3.1 Deterministic dynamics: effects of mortality 11

3.2 Stochasticity and loss of the stock-recruitment relationship 14

3.3 Stochasticity and signals of density dependence 16

4 DISCUSSION **18**

ACKNOWLEDGEMENTS **23**

DATA AVAILABILITY STATEMENT **23**

REFERENCES **24**

APPENDICES **30**

A Mathematical model **30**

A.1 Fish population dynamics 30

A.2 Plankton dynamics 33

B Partitioning mortality within cohorts **34**

C Parameter values **35**

1 INTRODUCTION

Small pelagic fish (e.g. anchovy) are striking for the lack of clear stock-recruitment relationships (SRRs) (Gilbert, 1997; Szuwalski et al., 2015; Hilborn et al., 2017). Abundance often varies unpredictably over several orders of magnitude from year to year (Schwartzlose et al., 1999; Hilborn et al., 2017). This variability is thought to be caused by changes in environmental conditions (Checkley et al., 2017). Numerous studies explain the weakness or absence of SRRs in small pelagic fish as a consequence of climatic fluctuations that affect survival from hatching to recruitment, so that recruitment is largely uncoupled from spawning biomass (Szuwalski et al., 2015). Such uncoupling stems from noise, rather than from a pattern of recruitment that remains unchanged as biomass increases, which would imply infinite compensation (Rose et al., 2001).

Usually, it is taken as granted that SRRs are the basic descriptors of density dependence limiting the abundance of fish stocks (Ricker, 1954; Beverton and Holt, 1957; Rothschild, 2000). The weakness of SRRs in small pelagic fish is therefore a serious issue, as it could lead to an inference that density-dependent constraints on population growth are weak or absent. However, it could alternatively be that the SRR is itself the problem (Andersen et al., 2017). For instance, body growth can be density-dependent beyond recruitment, and therefore not detected in the SRR (Lorenzen, 2008). Also, spawning biomass may not be a good reflection of egg production, if the latter depends on maternal feeding conditions (Takasuka et al., 2019b). In addition, random variation in the environment may hide SRRs, while leaving 'soft' floors and ceilings on abundance that regulate populations (Turchin, 1995)—the absence of an SRR does not imply an absence of density-dependent regulation.

SRRs have to emerge from density-dependent processes, and these processes are less well documented in small pelagic fish that fluctuate strongly in abundance, than in other marine fish (Takasuka et al., 2019a). MacCall (1980) suggested two basic mechanisms by which mortality could play a role in regulation of anchovy density. First, as large individuals become more abundant, their cannibalism on anchovy eggs and larvae may increase, restricting further population growth, leading to a Ricker-like SRR. In support of this, egg cannibalism has been reported widely since the late 1960s in several species of anchovy, such as *Engraulis japonicus, Engraulis mordax, Engraulis ringens, Engraulis capensis, Engraulis anchoita* (Hayasi, 1967; Hunter and Kimbrell, 1980; Alheit, 1987; Valdés-Szeinfeld, 1991; Pájaro, 1998; Pájaro et al., 2007). Cannibalism on anchovy larvae is less well documented, possible due to the short digestion time of the larvae stages (Hunter and Kimbrell, 1980). However, Pájaro and Ciechomski (1996) identified cannibalism on post-larval stages of *Engraulis anchoita*. Such cannibalism would occur when massive spawning takes place in areas where food is scarce (Pájaro et al., 2007). As a consequence, cannibalism operates as a density-dependent regulatory mechanism in anchovy populations (Pájaro, 1998).

MacCall's second mechanism brings together mortality and density-dependent body growth in the larval stage (MacCall, 1980). Slow body growth through a risky stage of life leaves fish vulnerable for longer, thereby increasing the risk of death before safer stages of life can be reached. If body growth slows down as larval density increases, or as plankton density decreases, then more death is accumulated. The mortality itself does not need to be density dependent—the important thing is that the mortality rate is greater during the period of slower density-dependent body growth. MacCall did not develop this, but the idea, which has its roots in a paper by Ricker and Foerster (1948), has been been central to theoretical and empirical research on recruitment in fish populations (Anderson, 1988; Sogard, 1997). Although evidence is scarce in anchovy, growth and survival during yolk absorption were reduced by low food availability in an experiment on *Engraulis mordax* (O'Connell and Raymond, 1970). Houde (1989), in a simulation study on *Anchoa mitchilli*, found density-dependent declines in larval anchovy growth rate as egg (or larval) density increased, stabilising recruitment levels. Also, simulations by Cowan et al. (1999) found that density-dependent effects on growth and survival, solely due to effects of anchovy on prey abundance, resulted in a dome-shaped relationship between adult production and the reduction in larval survival.

Density-dependent mechanisms also operate later in life, beyond the larval stage. Indeed, Anderson (1988) recognised that factors effecting growth and survival change as fish grow. Evidence of density-dependent growth was found in early studies of *Engraulis ringens* in Peruvian waters (Palomares et al., 1987). This showed that the growth performance index of juveniles and young adults, known as Φ, was negatively correlated with annual anchovy biomass from 1954 to 1982. These results confirmed previous findings by Jordan (1980) indicating a shift of anchovy maximum length as a consequence of changes in the growth rate. There is also evidence of food-dependent egg production in anchovy living in Tampa Bay, Florida (Peebles et al., 1996). As in other marine fish groups (Cowan et al., 2000; Stige et al., 2019), density dependence evidently can operate at multiple life stages in small pelagic fish.

Given the evidence for density-dependent processes in small pelagic fish, why are their SRRs so weak or absent? This paper is a numerical investigation of the problem, using a size-spectrum model (for background to these models, see Benoît and Rochet, 2004; Andersen and Beyer, 2006; Datta et al., 2010; Hartvig et al., 2011; Blanchard et al., 2014). Density dependence in somatic growth and reproduction is built into this modelling framework, so it can be used to examine the potential role (a) of growth through the larval stage, and (b) of competition for food for reproduction (MacCall, 1980; Takasuka et al., 2019a). Previous studies using size-spectrum models in this research area include analysis of the role of trophic interactions in generating SRRs in multispecies assemblages (Rossberg et al., 2013), effects of spatial dependence on the stage in life at which regulation of fish stocks could occur (Andersen et al., 2017), and exploration of whether strength of density-dependent growth in fish stocks is sufficiently strong to reduce optimal fishery size-at-entry to below size-at-maturity (van Gemert and Andersen, 2018).

Our results show that a SRR could emerge from the density-dependent processes in a deterministic setting. However, the addition of random fluctuations in the plankton can hide the signal of density dependence in the SRR, while leaving the density-dependent processes fully operational beneath this noise. In sum, a population can be both strongly regulated by density-dependent processes, and at the same time exhibit no relationship between stock and recruitment.

2 METHODS

Size-spectrum models provide a good platform on which to study density dependence encompassing body growth, because they contain the key couplings involving growth, that fish grow as a consequence of eating other organisms, and that fish die at least in part by being eaten. In addition, once maturity is reached, some part of incoming mass is transferred to reproduction, which makes births density-dependent as well. Importantly, no SRR needs to be assumed in these models—the dynamics decide internally what, if any, SRR emerges from the density-dependent processes, as happens in reality. This is the approach we take here. Models of multispecies, size-spectra dynamics have often imposed an SRR as an input (Scott et al., 2014), but it is not necessary to do so. (See also: Rossberg et al. (2013); Andersen et al. (2017)).

The framework for this study is a population of anchovy, chosen as an instance of an abundant, small, pelagic fish. The fish are supported by a size spectrum of autotrophic plankton, aggregated over taxa. Body growth is a central process in the fish size spectrum, but not in the plankton spectrum as these taxa are mostly unicellular. The dynamics of these two classes are therefore treated separately, and coupled together by feeding, and the deaths that follow from being eaten.

2.1 Fish population dynamics

The life history of a fish species entails growth in body mass w, and hence a size structure, which can be encapsulated in a function $\phi(w, t)$ describing the density of individuals as a function of their mass, often called a size spectrum. This is a density in volume as well as in mass, so $\phi(w, t)\mathrm{d}w$ gives the density in volume in a small size range $[w, w + \mathrm{d}w]$ at time t. The function unfolds over time through the action of births, growth and death (the vital rates), and can be described by a partial differential equation containing the key mechanisms affecting these vital rates, at simplest a size-based version of the McKendrick–von Foerster equation (Silvert and Platt, 1978). The main expressions used in the rate of change of density of fish are

as follows in this paper:

$$\frac{\partial \phi}{\partial t} = \underbrace{-\frac{\partial}{\partial w}\left[\tilde{\epsilon}\tilde{g}\phi\right]}_{\text{(a)}} - \underbrace{\tilde{d}\phi}_{\text{(b)}} - \underbrace{\tilde{\mu}\phi}_{\text{(c)}} + \underbrace{\epsilon_R \tilde{R}\frac{\tilde{b}}{w_{egg}}}_{\text{(d)}} . \tag{2.1}$$

We explain the notation and meaning of each term in the following paragraphs, and motivate them by means of the sketch in Fig. 1. Technical details are in Appendix A, starting with Eq. (A.1).

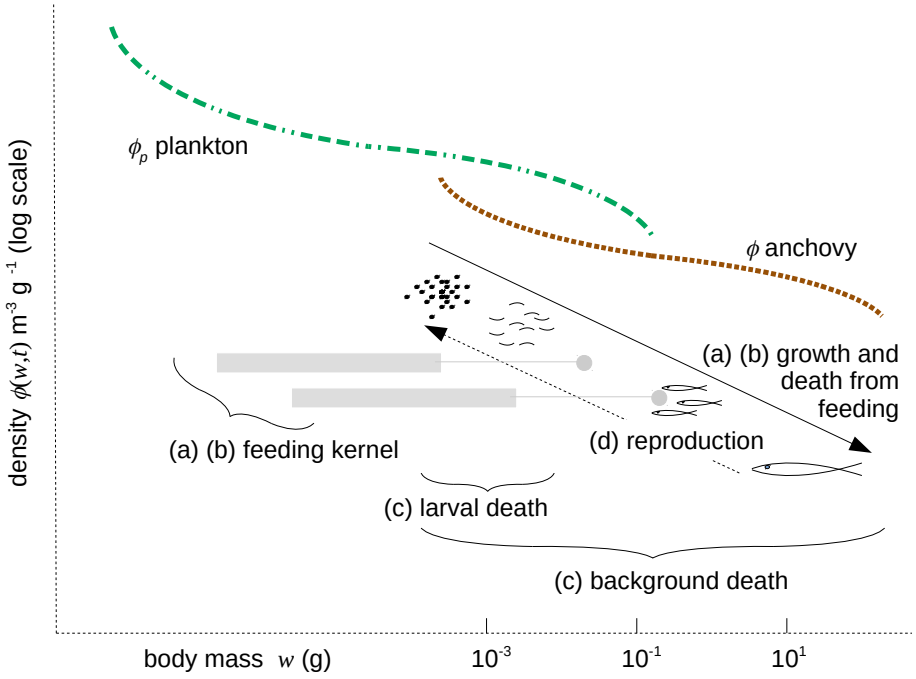

Figure 1: Sketch showing how to interpret terms (a), (b), (c) and (d) in the fish dynamics, Eq. (2.1). The equation operates at every body mass w in the size range of the fish population, and allows its density $\phi(w,t)$ (heavy dotted curve) to change over time. Body-mass values show the approximate location of anchovy in the scheme. The horizontal grey bars are two examples from a continuum of feeding ranges of anchovy, for a consumer at the size given by the connected circle; feeding leads to growth of the consumer (term a) and death of the prey (term b); additional causes of death are larval at small sizes (term c), and background at all sizes (term c). The population is replenished by reproduction (term d). Dynamics of the plankton size spectrum $\phi_p(w,t)$ (heavy dash-dot curve) are different, and are given in Eq. (2.2).

Term (a) deals with rates at which fish grow both into and out of the small mass range $[w, w + \mathrm{d}w]$. Term (b) deals with the death from cannibalism in this size interval. Terms (a) and (b) both contain a size-dependent feeding rate; this crops up in the per-capita death rate $\tilde{d}$ from cannibalism caused by larger anchovy

(Eq. (A.3)), and also in the rate $\tilde{g}$ at which mass accumulates from feeding on smaller organisms (Eq. (A.4)). The extra term $\tilde{\epsilon}$ partitions incoming mass between somatic growth and reproduction as the fish reach maturity (Eq. (A.8)), making $\tilde{\epsilon}\tilde{g}$ the per capita rate of somatic growth. Term (c) deals with intrinsic (density-independent) deaths in the same size interval (Eq. (A.7)), which we separate into two parts, to allow larval mortality (Eq. (A.5)) plus some background mortality (Eq. (A.6)). The rather complicated-looking term (d) simply turns the total rate at which reproductive mass, $\tilde{R}$, is generated into a rate at which eggs appear at the smallest mass w_{egg} (Eq. (A.9)). Note that, for clarity we have suppressed the arguments of the tilde-functions: in fact they all depend on body size (except for $\tilde{R}$). In addition, $\tilde{g}, \tilde{d}$ and $\tilde{R}$ are density-dependent; since density is the state variable, this makes them functions of time as well. We also include a diffusion term (Datta et al., 2010), not shown in Eq. (2.1), which allows growth trajectories of fish to spread out as the fish grow (see Eqs (A.1), (A.10)).

At the heart of the model is a dimensionless feeding kernel that allows the gain in body size of a consumer to be coupled to death and body size of the prey it eats. This makes births, growth and deaths density-dependent, for the following reasons. First, mature fish have more resources to allocate to reproduction when food is plentiful, and less to allocate when food is scarce. Secondly, when food is plentiful, the fish grow relatively fast; when food is scarce, they grow more slowly. Thirdly, when larger fish (cannibals) are abundant, the death rate from cannibalism is relatively high; when larger fish are scarce, this death rate falls. The shape of a feeding kernel is a biological matter. Anchovy, being a planktivore, feeds mostly by filtering water through gill rakers, although it can also feed as an active predator when large (Espinoza and Bertrand, 2008). We use a kernel that is unselective within a given size range (Eq. (A.2)), to reflect the filter feeding. The per-capita death rate from cannibalism $\tilde{d}$ then takes the feeding kernel, multiplies density of cannibals, and sums over all cannibal sizes (Eq. (A.3)). This summation contains a weighting that scales with cannibal size, on the grounds that larger fish filter a greater volume of water per unit time. The flip side of this death process is the growth $\tilde{g}$ that comes from feeding, which can in principle include both small anchovy and plankton (Eq. (A.4)). The contribution from cannibalism to the food of anchovy is set by a parameter θ (Eq. (A.4), also in Eq. (A.3)). $\theta = 0$ switches off cannibalism, and $\theta = 1$ makes feeding indiscriminate with respect to cannibalism and planktivory. Anchovy feed on plankton under all circumstances.

Mortality from cannibalism above is dynamic and changes with time because it depends on the abundance of larger fish. In addition, we introduce a fixed larval death rate to represent the special vulnerability of the larval state. This is taken to be a reverse-sigmoid function, starting high at egg size and tending to zero as the fish leave the larval stage (Eq. (A.5)). We also include a fixed background mortality that decreases as body mass increases over most of the size range of anchovy, but starts to increase again, as the fish get near to the asymptotic mass (Eq. (A.6)). The decrease is in keeping with slower dynamics of larger organisms, and the increase near the largest body size is a device to prevent a build-up of density at body sizes

invulnerable to other causes of death. The increasing component can be thought of as predation by larger taxa that would in reality be eating them, or simply as a term describing senescence. Summing the two fixed death rates (Eq. (A.7)), gives the per-capita death rate $\tilde{\mu}$ used in Eq. (2.1). Together with cannibalism, the death terms generate a U-shaped mortality schedule for the life history as a function of body size (Hall et al., 2006).

Reproduction depends on the proportion of incoming mass partitioned to reproductive activities, given by a function $1 - \tilde{\epsilon}$ (Eq. (A.8)). This function allows gradual maturation of the fish, and also allows an increasing proportion of incoming mass to go to reproduction after maturation. The proportion reaches unity at the maximum body mass because, at this point, there is no further somatic growth; this defines the upper limit of the size spectrum. Using the function $1 - \tilde{\epsilon}$, the total population rate $\tilde{R}$ at which reproductive mass is created is obtained as a summation over body size (Eq. (A.9)). The total mass rate $\tilde{R}$ is then partitioned into a number density rate at which eggs appear, using the function $\tilde{b}$, allowing for some inefficiency ϵ_R. We simply assume that eggs are all the same size w_{egg}, and this sets the smallest body size in the size spectrum.

2.2 Plankton dynamics

Density-dependent body growth of fish requires that less food —here mostly plankton— should be available as population density increases, so that body growth slows down. The plankton dynamics have therefore to be specified. Plankton themselves form complicated, multispecies, size-structured assemblages, simplified here to a continuum of cell sizes (a size spectrum), with dynamics specified at each size, as in earlier size-spectrum models (e.g. Hartvig et al., 2011). Over most of this size range, the plankton are unicellular, and we therefore assume that plankton populations increase directly by cell division without somatic growth. The absence of somatic growth calls for a modelling framework quite different from the McKendrick–von Foerster equation above (Eq. (2.1)). Typically a linear semi-chemostat dynamic has been assumed in the size-spectrum literature, to account both for local population dynamics and also for invasions from outside (Hartvig et al., 2011). We make these two processes explicit here, using a local logistic dynamic plus an immigration term. Population growth rate can then potentially decline as density falls (depending on the rate of immigration), rather than always tending to its maximum value.

The plankton size spectrum is given as a function $\phi_p(w, t)$ of cell size w, changing over time through its own dynamics and through its interactions with anchovy. The rate of change of density at body mass w is written as:

$$\frac{\partial \phi_p}{\partial t} = \underbrace{\tilde{r}\phi_p\big(1 - \phi_p/\tilde{a}\big)}_{\text{(a)}} + \underbrace{\tilde{i}}_{\text{(b)}} - \underbrace{\tilde{d}_p\phi_p}_{\text{(c)}}. \tag{2.2}$$

The motivation for the terms in Eq. (2.2) is given below; technical details are in Appendix A, starting with Eq. (A.11). (Note that parameters $\tilde{r}$, $\tilde{a}$ and $\tilde{i}$ are all

functions of cell size (Eqs (A.12)). Term (a) is the basic logistic dynamic that would ultimately lead an isolated plankton assemblage to a size spectrum corresponding to the carrying-capacity (equilibrium-density) function, $\tilde{a}$, in a deterministic setting. How rapidly plankton of different cell sizes get to equilibrium depends in part on the function $\tilde{r}$ describing the intrinsic rate of increase. Term (b) is an immigration rate, independent of local dynamics, that replenishes the plankton, and allows some control over the sensitivity of the plankton to planktivory. Term (c) is the effect of planktivory on the plankton spectrum. The function $\tilde{d}_p$ is the per-capita death rate of plankton at cell mass w from feeding by anchovy (Eq. (A.13)). This is similar to cannibalism (Eq. (A.3)), being a function of anchovy body-size and density, and therefore a function of time.

2.3 Numerical methods

In fisheries science, SRRs are obtained from time series of spawning biomass and recruitment. We took the same approach for obtaining SRRs in the model, constructing time series of the anchovy-plankton system, solving the partial differential equations (2.1), (2.2) by numerical integration. Prior to doing this, the equations were transformed to a logarithmic scale of body size, $x = \log(w/w_0)$, where w_0 is an arbitrary constant, as described in Appendix A (see Eqs (A.1), (A.11)). This transformation was used because cell and body mass span about twelve orders of magnitude in the model. Parameter values for the equations were motivated as far as possible by knowledge of anchovy and plankton, as described in Appendix C.

Unless otherwise stated, the equations were discretised into small size steps $\delta x = 0.1$, and numerical integrations were done on the resulting system of ordinary differential equations. Such equations operate in continuous time, and were solved numerically with a step size $\delta t = 0.001$ yr (unless otherwise stated), using the Euler method. The speed of computation was increased by applying fast Fourier transforms to the convolution integrals in Eqs (A.3), (A.4), (A.10) and (A.13). Numerical integrations were initiated with arbitrary size structures, and were allowed to relax to a more natural state over the first ten years. At this point, the anchovy size spectrum was reduced by a factor 10^7, without altering the current size structure, and then allowed to recover. The purpose of this was to allow a large change in density from which signals of SRRs could be extracted when the dynamics were deterministic.

Because the model operates in continuous time, it was not structured in cohorts appearing say once a year. However, the growth trajectory of cohorts of individuals born at the same time is given approximately by the solution of a differential equation

$$dx/dt = \epsilon(x)g(x,t), \tag{2.3}$$

from an initial condition set as the logarithm of egg mass at time 0, where $\epsilon(x)$ and $g(x,t)$ are defined in Eq. (A.8), (A.4) respectively (Law et al., 2009; Datta et al.,

2010). We obtained numerical solutions of this differential equation to follow the growth of cohorts.

To generate a random environment for anchovy, the carrying-capacity function of the plankton was turned into a random variable, altered at half-year intervals. This was done by multiplying the carrying-capacity function $a(x)$ (Eq. (A.12)) by a random factor, uniformly distributed on a logarithmic scale, over a range from about half to double the baseline value. The same factor was applied at all plankton cell sizes, thereby moving the whole function up and down. This created better or worse conditions for plankton, to which they rapidly responded. This in turn generated more food or less food for anchovy, and correspondingly faster or slower body growth, leading to fluctuations in anchovy biomass over time similar in magnitude to those observed in the sea (Hilborn et al., 2017). We took a 25 yr time period to construct SRRs starting in year 15, taking a single measurement each year, in keeping with the way in which these relationships are constructed in practice. The random variable above generates white noise in the log of the carrying capacity. As there is evidence for both red and white noise (Di Lorenzo and Ohman, 2013), we did a check that the results were not dependent on the white noise, using the discretisation of the Ornstein-Uhlenbeck process to generate a reddened noise spectrum.

The numerical analysis was carried out using code written in C. As an independent check, the key computations were repeated independently in the R software package Mizer (Scott et al., 2014), without the diffusion term in Eq. (A.1). The mizer code and results are available at `https://rpubs.com/gustav/plankton-anchovy`.

3 RESULTS

3.1 Deterministic dynamics: effects of mortality

To show how cannibalism and larval growth (MacCall, 1980) can affect dynamics of small pelagic fish, we introduce them in a stepwise manner into a model system based on Eqs (A.1), (A.11), with parameter values as in Appendix C, Tables 1, 2. These equations describe how density (or biomass density), expressed as a function of body size (i.e. a size-spectrum), unfolds over time. It is important to keep in mind that the dynamics give the time evolution of these whole size spectra, although we collapse them to total population biomass densities in the graphs below. To emphasize this point, Fig. 2a shows an example of biomass-density functions of plankton and anchovy at a particular time; aggregated measures are constructed from functions like these.

The first step just puts in place a baseline comprising planktivory and fixed background mortality (Fig. 2b). As the anchovy population builds up, it causes

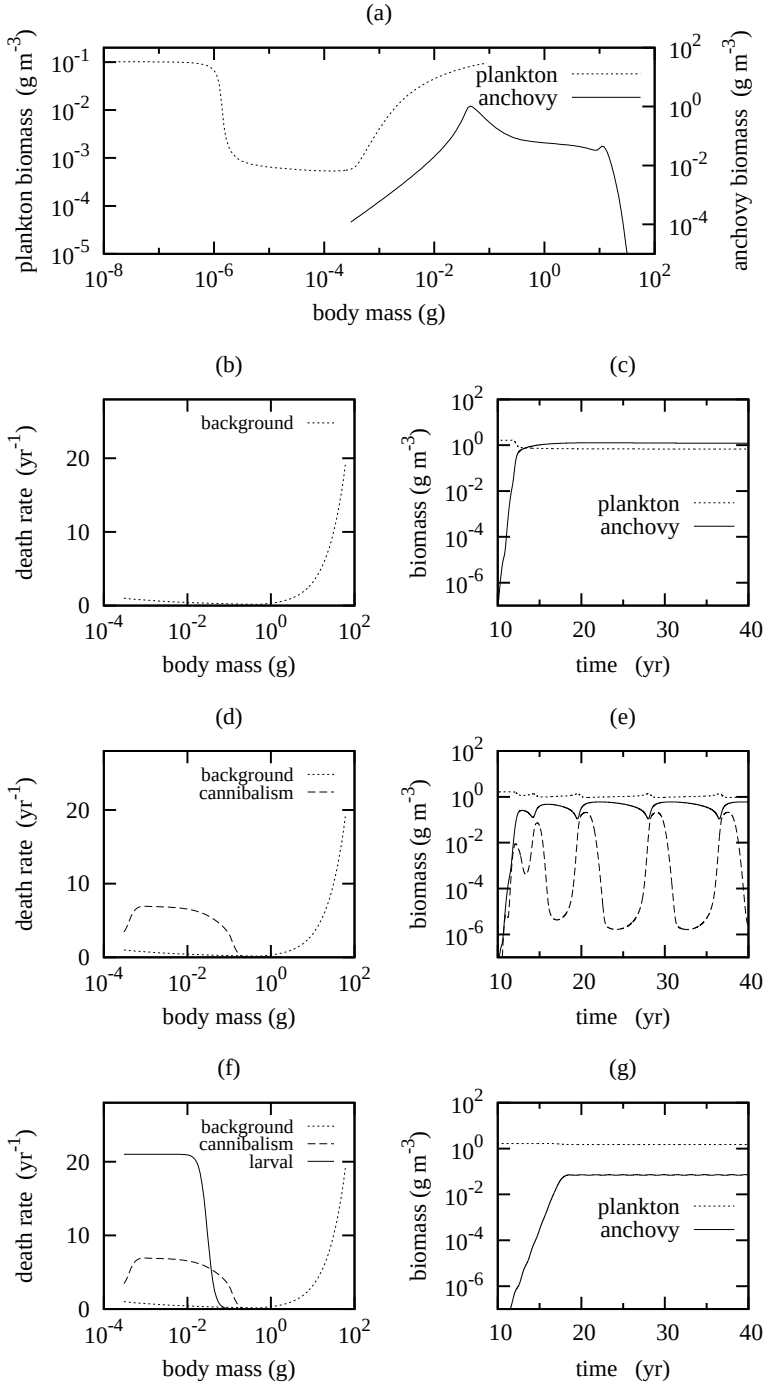

Figure 2: Changing size-spectrum dynamics as cannibalism and larval mortality are added to a baseline model. The state variables are plankton and anchovy size spectra, illustrated at one point in time in (a). (b), (c) Baseline in which anchovy feeds on plankton with background mortality present. (d), (e) Baseline + cannibalism. (f), (g) Baseline + cannibalism + larval mortality. (b), (d), (f) Size-specific death rates. (c), (e), (g) Time series of total biomass densities, obtained by summing over the size ranges in which feeding occurs at each time. Dashed line in (e) is biomass density of anchovy summed over a small size range 0.01 to 0.4 g. Background and larval mortality are fixed over time; cannibalism changes as anchovy abundance changes and is shown at the start of year 30 in (d) and (f). Size spectra in (a) are those at the start of year 30 in (c).

a large reduction in part of the plankton spectrum, and a corresponding large reduction in the rate of somatic growth of anchovy that feed on these plankton. This is great enough to stop the anchovy population from increasing (Fig. 2c). The effect on the biomass spectra can be seen in Fig. 2a, illustrated in year 30, after the anchovy population has stopped increasing. The peak in biomass here is caused by a bottleneck due to slow somatic growth. Evidently, density-dependent growth of individuals can constrain population increase, even without invoking extra larval mortality. The fall in somatic growth here is too great to be realistic, but we show below that, once cannibalism and larval mortality have been incorporated, the growth trajectories that emerge are realistic for anchovy.

The second step introduces cannibalism by a single change to the cannibalism parameter θ: $0 \to 1$ (Fig. 2d). Feeding by anchovy then no longer discriminates between the plankton and anchovy of the same size. The effect is to generate oscillations in abundance of anchovy (Fig. 2e). The fluctuations in total biomass mask much larger oscillations taking place in a restricted part of the anchovy spectrum, shown as the dashed line in Fig. 2e. The extra mortality from cannibalism fluctuates over time, and is shown at the start of year 30 in Fig. 2d (also in Fig. 2f).

The third step introduces an additional high rate of larval mortality (Fig. 2f). This is constant over time, and acts as a brake on anchovy population growth, holding it at lower population densities (Fig. 2g). There are two effects of this: first the effect of anchovy on plankton is smaller; secondly it changes anchovy's per capita death rate from cannibalism. The consequences for the dynamics are far reaching, damping the oscillations caused by cannibalism (Fig. 2e), as illustrated in Fig. 2g. As larval mortality increases, damping becomes stronger; we used a death rate at birth of $l_{\underline{l}} = 21$ yr^{-1} (Fig. 2f), close to the smallest value that would stabilise the dynamics.

A realistic trajectory for somatic growth of anchovy cohorts (Fig. 3a) emerges from the dynamics described in Fig. 2f, g. The trajectory was constructed from the time series in Fig. 2f, g, and gives maturation around 10 g, at an age of about 1 year. Note that growth curves of cohorts are dynamic features of size-spectrum models that emerge from feeding (Eq. (A.4)); they are obtained by solving Eq. (2.3), and are independent of any assumed model of growth. The trajectory motivates a SRR based on recruitment at 10 g as a function of the spawning-stock biomass one year earlier. For much of the time the SRR sits near a single point, because the population was close to equilibrium by year 20. But the early period of population growth is sufficient to show the emergence of a SRR (Fig. 3b). The SRR has some resemblance to the Beverton and Holt equation, because the approach to equilibrium is nearly monotonic (Fig. 2g). But emergent SRRs also depend on the shape of the initial size spectra, and could be much more complicated in time series with damped or sustained fluctuations, unlike the standard forms usually assumed.

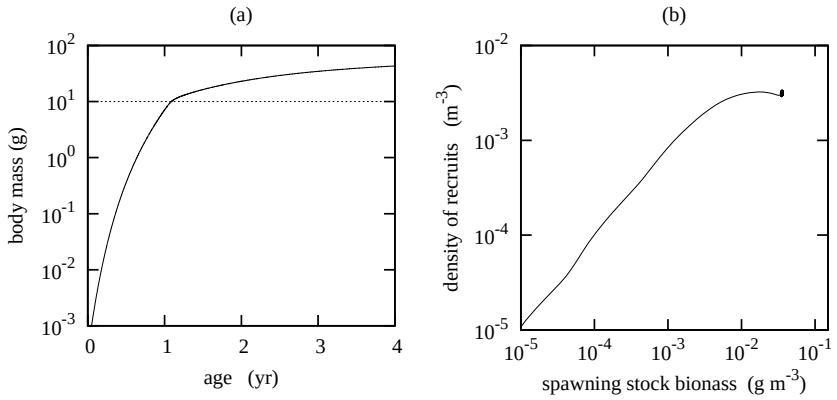

Figure 3: An emergent stock-recruitment relationship, with a time lag of 1 year from egg to recruitment at 10 g. (a) Somatic growth of a cohort born at the start of year 30 shows that it takes ∼1 year to grow from egg to 10 g (horizontal line). (b) Density of recruits, as a function of spawning stock biomass one year earlier. The graphs were constructed from the example shown in Fig. 2f, g.

3.2 Stochasticity and loss of the stock-recruitment relationship

The model in Section 3.1 builds several core processes into anchovy population dynamics, namely: plankton dynamics, planktivory, cannibalism, somatic growth, reproduction, and death (background, larval, cannibalistic). However, it is still missing the large, irregular fluctuations over time, characteristic of small pelagic fish (Schwartzlose et al., 1999). We therefore make the plankton a random variable. Stochasticity could be introduced in many different ways. Here the carrying-capacity of plankton in Eq. (2.2) was transformed into a random variable, as described in Section 2.3. In other respects, the system was as in Fig. 2f, g. Since this generated white noise, we also checked that similar fluctuations could be generated by a reddened noise spectrum.

Random variation in the plankton causes fluctuations in anchovy (Fig. 4a), which has its own inbuilt tendency to oscillate. The relationship between spawning stock biomass and recruitment one year later is plotted as Fig. 4b. Consistent with empirical studies on small pelagic fish (Szuwalski et al., 2015), there is little sign of a relationship between stock biomass and recruitment. We used a time lag of one year for recruitment because the fish grew to the region of 10 g by then (Fig. 3a), but note that random fluctuations in the plankton food can lead to considerable variation in the age at which they reach this size. Similar results were obtained when the random variation had a reddened noise spectrum (Fig. 4c, d).

The random fluctuations in plankton illustrate how density-dependent body growth and larval mortality can work together to regulate a population (MacCall, 1980). Fig. 4e shows the growth of two nearby cohorts from the time series in

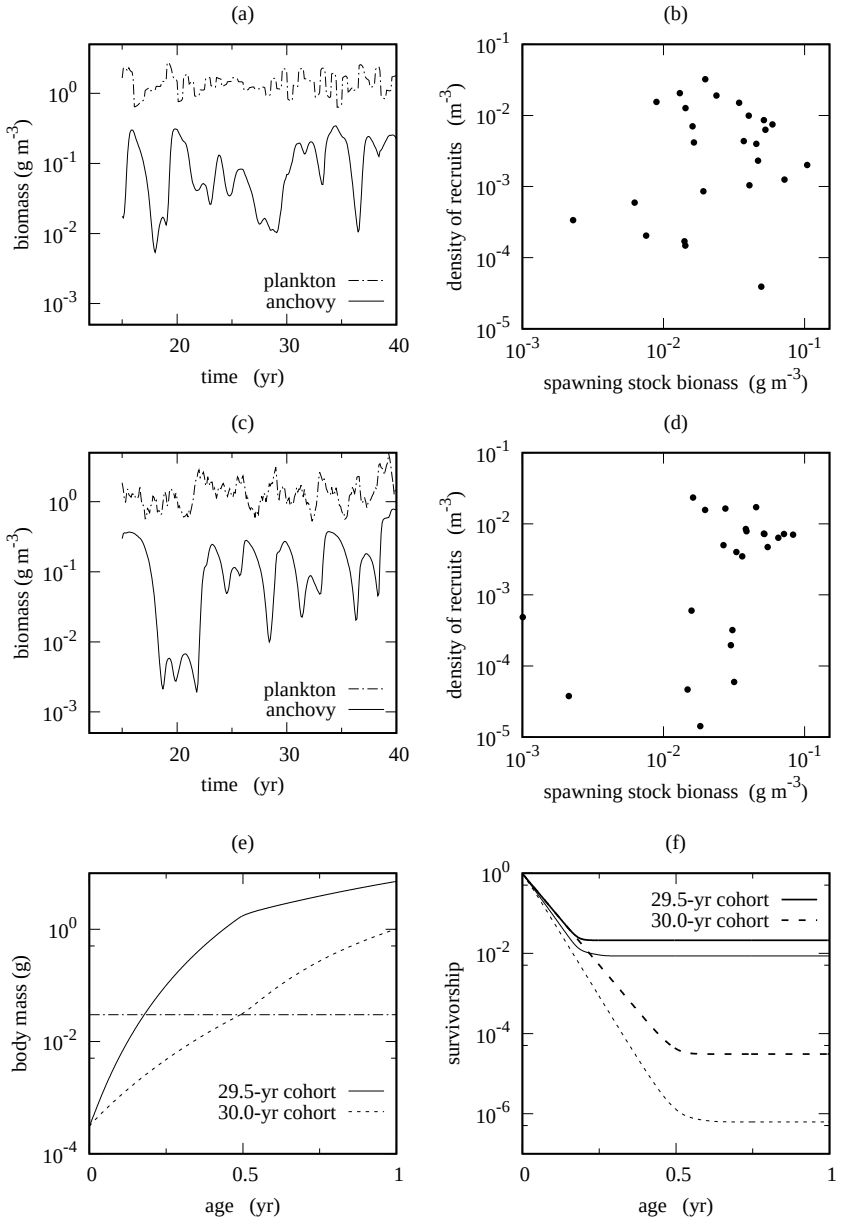

Figure 4: Absence of a stock-recruitment relationship with random variation in plankton. (a) Time series obtained by adding white noise to the system shown in Fig. 2f, g; the time series starts at 15 yrs, after recovery of the anchovy population. (b) Relationship between spawning stock biomass and density of recruits at size 10 g 1 year later, plotted once a year, starting in year 16. (c), (d) Plots as (a), (b), but with red noise instead of white. (e) Growth of two nearby cohorts with contrasting amounts of food, born at time 29.5 and 30.0 years in (a); the horizontal line marks the body size around which the fish leave the larval stage. (f) Proportion of individuals in the two cohorts surviving to each age (survivorship); the sources of mortality used for survivorship are: larval mortality (heavy lines), and larval mortality + cannibalism (light lines).

Fig. 4a, one born at time 29.5 years, when plankton were relatively abundant, and the other born at time 30 when plankton were relatively scarce. The horizontal line in Fig. 4e shows the body size (0.03 g) around which emergence from the larval stage happens (Appendix C): the more limited supply of food in the year-30 cohort approximately doubles the age at which this cohort is able to escape from high larval mortality. Consequently, the fish are vulnerable to mortality at the larval stage for longer, and fewer survive to become juveniles, evident as the age at which the survivorship curves become less steep in Fig. 4f. Survivorship can be partitioned into its components of cannibalism and larval mortality (see Appendix B), and we show separately the component from larval death and the combined larval mortality + cannibalism in Fig. 4f. Fixed background mortality is small at this stage in life and is not included (Fig. 2f). Survivorship from larval mortality was about 2.5 orders of magnitude greater in the faster-growing cohort by the end of the larval stage, and survivorship from aggregated larval mortality + cannibalism was about 4 orders of magnitude greater. This mechanism of density-dependence is potentially a powerful means of population regulation.

3.3 Stochasticity and signals of density dependence

Although a SRR is no longer evident when the plankton environment is a random variable (Fig. 4b), the system was identical to the deterministic one that gave a clear SRR (Fig. 3b), except for the added stochasticity in the plankton. So all the density-dependent processes were still fully operational, and strong signals of density dependence at the lower level of vital rates can still be detected in the presence of random variation in plankton. We show this first for the larval mechanisms of density dependence (MacCall, 1980), and secondly for mechanisms of density dependence that operate later on in life (Andersen et al., 2017).

As an instance of the first mechanism of density dependence through cannibalism (MacCall, 1980), Fig. 5a shows a clear relationship between the per capita death rate of eggs from cannibalism and the biomass of anchovy that eat eggs. These values were taken from the time series in Fig. 4a, b, at the start of each year, beginning in year 15. Although the relationship is clear, it does contain some noise. This is because a given biomass of cannibals can be obtained from a variety of cannibal size spectra. Since cannibals of different sizes have different effects on death rate of their prey (Eq. A.3), the death rate changes to some extent as the shape of the anchovy size spectrum fluctuates in the random environment.

MacCall's second mechanism, combining density-dependent growth with mortality (MacCall, 1980), is more intricate. To examine this, we extracted from the time series in Fig 4a, b, a sequence of cohorts, born at the start of each year, beginning in year 15. In each cohort, we followed body growth and the accumulated mortality up to an age of 0.4 years, this age being guided by the fast- and slow-growing cohorts in Fig 4e and the survivorship curves in Fig 4f. The faster the growth, the larger the fish would be by 0.4 years. Also, the faster the growth, the

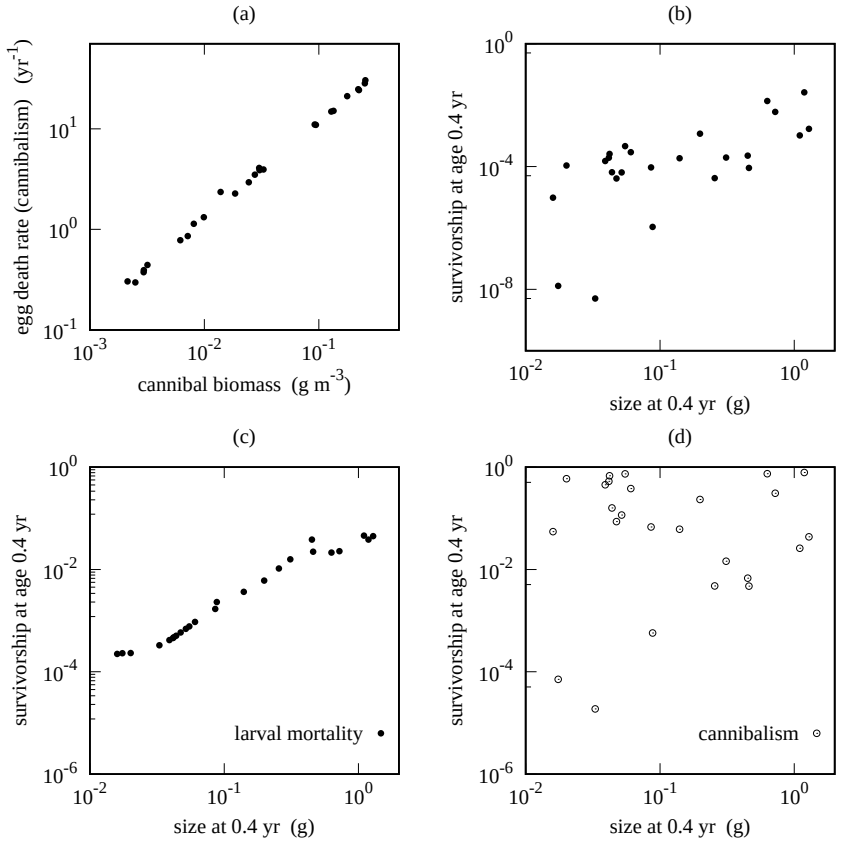

Figure 5: Signals of density dependence early in the life of anchovy living in a stochastic environment. (a) Egg death rate from cannibalism increases with the biomass of anchovy that eat eggs. (b) Cohort survivorship at age 0.4 yr increases with growth rate through the larval stage. (c) Component of cohort survivorship from larval mortality. (d) Component of survivorship from cannibalism. Cohorts were extracted at the start of each year from the time series on which Fig. 4 a, b was based, beginning in year 15.

earlier the escape from the larval stage, and the lower the accumulated mortality by age 0.4 years. Thus Fig. 5b shows a positive relationship between survivorship to age 0.4 years and body size at this age, as required by McCall's mechanism. It does however contain a lot of noise. To see where the noise comes from, it helps to disaggregate the contributions of larval mortality and cannibalism to the survivorship (Appendix B explains how this can be done). The signal from larval mortality is strong (Fig. 5c), but the signal from cannibalism is weak (Fig. 5d). Fig. 5b is essentially a product of these two survivorships, because the only other cause of death (background mortality) was small at this stage in life. Therefore, cannibalism was largely responsible for the noise, its fluctuations over time being uncoupled for the most part from the current biomass of plankton on which growth of larval anchovy depends.

Importantly, density dependence is not confined to early stages in life: it is pervasive through the whole life history because all growth depends on availability

of food. To illustrate this, Fig. 6 shows the dependence of mass-specific growth rate on the biomass of food available to anchovy at body size 1 g (Fig. 6a), and at 15 g shortly after maturation (Fig. 6b). As food goes down, so does growth. After maturation, this also means that there is less food to allocate to reproduction (open squares in Fig. 6b), so reproduction is density-dependent, just as somatic growth is. Note that no variation is created by fluctuations in the prey size spectra (c.f. Fig. 5a). This is because the integral on which the growth rate depends (Eq. (A.4)) is directly proportional to the food biomass, in the case of a box-shaped feeding kernel. We increased the precision of the numerical integration for Fig. 6, to show this.

However, the clear signal of density dependence in mass-specific, reproductive allocation (open squares at body size 15 g in Fig. 6b) is weakened by aggregating over the population to get the total rate of egg production. First, the mass-specific rate has to be multiplied by the biomass density of anchovy at 15 g to get the population rate of allocation to reproduction at 15 g. This biomass carries a longer history of random events in the plankton, which generates variation between cohorts in feeding and growth in anchovy before they reach this size. The biomass also carries the effects of anchovy's inherent tendency to fluctuate (Fig. 6c). These processes introduce noise into direct relationship between current feeding conditions and the contribution to reproduction at 15 g. Secondly, the total allocation to reproduction of the population (and hence total rate of egg production) brings together the variation between cohorts at all adult body sizes (Fig. 6d). In this way reproduction becomes uncoupled from current feeding conditions, and it would be optimistic to expect to see a strong signal of density dependence remaining. A positive signal is left between egg production rate and spawning biomass, but this does not involve a negative feedback, and does not contribute to regulation of the population (results not shown).

4 DISCUSSION

The basic message from this numerical study is that population regulation of small pelagic fish can operate without generating a SRR. This suggests that a SRR may not be the best place to look for evidence of density dependence. At the fine level of vital rates (birth, growth, death), density dependence was built into our model, irrespective of whether the plankton was deterministic or stochastic. A SRR would need to emerge from these density-dependent processes, since no SRR was imposed by the model. In a deterministic environment, a relationship resembling a Beverton-Holt SRR did indeed emerge from our model, as parameterised for anchovy. (This is not to suggest that such a relationship would be found in general: the range of emergent SRRs is potentially much richer than the Beverton-Holt and Ricker equations would allow, as Rossberg et al. (2013) observed in a multispecies size-spectrum model). However a random plankton environment can disturb size spectra in ways that mask the effects of density dependence, so that little trace of

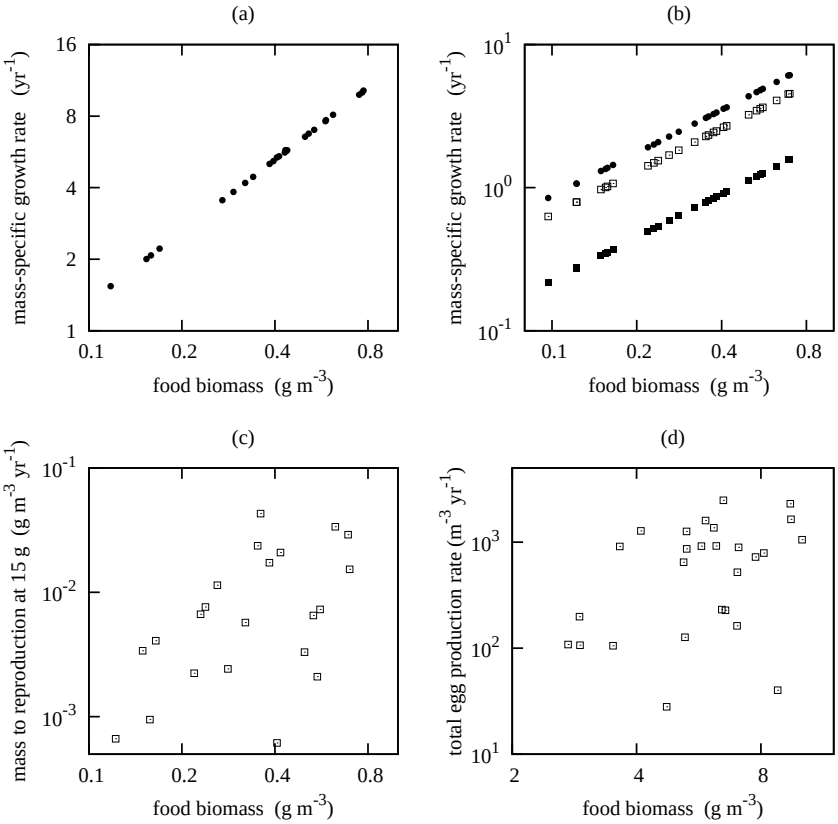

Figure 6: Signals of density-dependence in juvenile and adult anchovy living in a stochastic environment. (a) Mass-specific growth rate at 1 g. (b) Mass-specific growth rate after maturation at 15 g; here the total rate (filled circles) is partitioned into somatic growth (filled squares), and reproduction (open squares). Growth rates were calculated from the feeding kernels at the given body sizes, and included food both from plankton and from small anchovy. (c) Total population rate at which incoming mass is allocated to reproduction at 15 g. (d) Rate of egg production summed over all adult body sizes. Measurements were taken at the start of each year from the time series on which Fig. 4a, b was based, beginning in year 15. Integrations were run with $\delta x = 0.025$, and $\delta t = 0.0002$ for precision.

a SRR is left, despite the density-dependent processes still being fully operational. A population can both be strongly regulated by density-dependent processes and, at the same time, show little or no relationship between stock and recruitment.

Much of the core density dependence in the model comes from the action of fish growing by eating other organisms, and dying in part by being eaten. This makes growth a quadratic function of density at the level of the population, because it depends on a product of food density and consumer density. A mass-specific growth rate removes the consumer mass density, but the food mass density stays in place, so the mass-specific growth rate remains density-dependent (Eq. A.4). Density-dependent body growth is not a standard part of fisheries modelling (Lorenzen, 2016), and it has taken the size-based McKendrick–von Foerster equation and related models to bring it to the heart of population dynamics (Benoît and Rochet, 2004; Andersen and Beyer, 2006; Datta et al., 2010; Blanchard et al., 2014). These size-based models generate a much richer set of density-dependent feedbacks, including those between food availability and body growth and reproduction. The feedbacks are consistent with the empirical evidence of density dependence in growth, nutritional condition, maturation and reproductive parameters of fish (Cowan et al., 1999; Rose et al., 2001; Lorenzen and Enberg, 2002; Skjæraasen et al., 2012; Svedäng and Hornborg, 2015; Takasuka et al., 2019a).

MacCall (1980) envisaged two density-dependent mechanisms at the egg and larval stages that could regulate anchovy, first cannibalism, and secondly slow growth that would prolong a period of high larval mortality. Both of these are connected to density-dependent feeding in anchovy, and both contribute to the feedbacks in the size-spectrum model used here (Fig. 5). Moreover, density dependence extends beyond the larval stage, as illustrated in Fig. 6, because growth continues throughout life (Lorenzen, 2008; Takasuka et al., 2019a; van Gemert and Andersen, 2018). However, cannibalism on its own is not a process that helps to stabilise anchovy in our system (Fig. 2e). Although cannibalism can generate stable size spectra under certain conditions, to do so it needs some conspecific prey to be close to the consumer size, to provide short enough feedback loops and time delays (Plank and Law, 2012). Planktivores filter-feed low down in the food chain, and are unlikely to meet this requirement. We set the largest prey mass at 1/100 that of the consumer, large enough to allow some feeding beyond the plankton by adult anchovy (Espinoza and Bertrand, 2008). But this still allowed large oscillations in the absence of compensating mechanisms (Fig. 2e). (In an earlier paper with different model assumptions, we set the ratio at 1/10, and this did usually stabilise the dynamics (Canales et al., 2016).) If a large separation between prey and consumer size is a general feature of planktivory, cannibalism is unlikely to contribute to planktivore regulation, even though it is density dependent. As Turchin (1995) pointed out, density dependence is a necessary, but not sufficient, condition for regulation.

Where do the signals of density dependence, so clear at the fine level of growth and death rates, get lost in the SRR of a random environment? One clue lies in the partition of survivorship between fixed larval mortality, which left the signal largely intact (Fig. 5c), and cannibalism, which introduced a lot of noise to the signal (Fig.

5d). Survivorship from cannibalism is rather uncoupled from random variation in plankton that determines how fast anchovy larvae grow. There are two reasons for this. First, cannibals, being much older and larger than the larvae, had also been influenced by random conditions at earlier times, as well as by the current state of the plankton. Secondly, fish populations have their own inherent tendency to fluctuate, and cannibalism is itself a potential driver of these oscillations (Fig. 2e). Random changes to the plankton may be needed to get the fluctuations started, but there is no obvious reason why the fluctuations should then synchronise themselves to the plankton. (The period of oscillations from cannibalism did get longer as somatic growth rate went down; results not shown here.) Fluctuations in abundance are known to be particularly large in small pelagic fish (Schwartzlose et al., 1999; Hilborn et al., 2017), and could help mask the signal of density dependence in mass-specific growth. Further weakening of the SRR could come from random variation in the larval mortality (we held it fixed), and larval mortality from predation by other species, with dynamics that are also uncoupled from the random plankton. These are just a few of the many ways in which a signal of density dependence could be weakened on the path to a SRR.

On the other side of the coin, what conditions might favour the emergence of SRRs? Clearly, less variability in processes uncorrelated with driving variables such as plankton food would help. Thus SRRs are more likely to be seen in fish species with life histories that generate relatively small fluctuations in abundance. This includes behaviour that permits feeding on at least some conspecific prey relatively close to the predator body size. Such feeding promotes stability of size spectra (Plank and Law, 2012), in contrast to the planktivorous feeding by small pelagic fish. Also, certain life-history traits lead to less fluctuation, including long life, in particular long adult life, and repeated spawning (Murphy, 1967; Hsieh et al., 2010). This consistent with the existence of SRRs in some long-lived species of the Gadiformes (Szuwalski et al., 2015). However, human exploitation is a potential driver of fluctuations (Essington et al., 2015); truncation of age and size structures by preferentially removing fish that are large for their species could contribute to this (Hsieh et al., 2010). So it could be that exploitation of fish stocks is a further reason why SRRs can be hard to observe.

What are the implications of these results? Clearly, the role of density dependence in management of fish stocks is important to understand, because it offsets losses of individuals, from anthropogenic activities such as fishing, and from natural fluctuations in environmental conditions (e.g climate, predators) (Rose et al., 2001). Models of SRRs directly affect estimates of biological reference points (Takasuka et al., 2019a), and are currently at the core of fishery management based on maximum sustainable yield. However, attempts to document density dependence in small pelagic fish through standard SRRs have been largely unsuccessful (Szuwalski et al., 2015), and this paper shows some reasons why this should be so. Yet, beneath the noise, density-dependent processes can remain fully operational and measurable, at the level of vital rates of birth, growth and death. Thus the main implication of our results is that it might be better to look for the signals of den-

sity dependence closer to the vital rates themselves, before they are scrambled by processes weakly correlated with density dependence.

This work is essentially a numerical example, structured as far as possible to match the life history of a small pelagic fish species (anchovy). The model encompasses several core population processes, including plankton dynamics, planktivory, cannibalism, somatic growth, reproduction, and death (background, larval, cannibalistic), but is still a simplification of processes operating in the sea. First, for simplicity, neither plankton food nor anchovy population dynamics were seasonal; it would be feasible to investigate this (Datta and Blanchard, 2016). Neither does the stochastic plankton model deal realistically with fluctuations, such as the El Niño/La Niña oscillations and decadal-scale shifts (Salvacetti et al., 2018); we have simply used random variation in plankton to generate fluctuations of anchovy similar to those observed empirically. Secondly, in reality, anchovy is embedded in a multispecies fish community. Predation by other species is important and will be included in future work. To some extent, the fixed larval and background mortality we used acts as a placeholder for predation mortality by other species; including other species explicitly would probably mask the SRR still further. Thirdly, we made a compromise over the feeding kernel, moving its lower limit to keep it a fixed proportion of the body size of the fish. This was a technical assumption, made for computational efficiency, as it allowed a fast Fourier transform on the convolution integrals. An alternative assumption would be to allow feeding kernels to get broader as planktivores get larger, spreading feeding over a greater range of plankton, and weakening the effect of anchovy on plankton of a specific size (Canales et al., 2016), but this would have been costly in computational terms. The dynamics of size-spectrum models are affected by the choice of feeding kernel, and aligning kernels more closely to observed feeding behaviour would be helpful in future work. Fourthly, the level at which larval mortality was fixed, while consistent with information available (Contreras et al., 2017), placed the anchovy close to the point of bifurcation between a stable equilibrium and an oscillatory solution in the deterministic dynamics. As a result, fluctuations in anchovy in the stochastic system were large, although still consistent with those observed in practice (Schwartzlose et al., 1999). We also assumed the law of mass action, setting interactions proportional to densities averaged over space. Spatial variation in densities could have important effects on the dynamics (Andersen et al., 2017); the problem is deciding what to replace the law of mass action with.

ACKNOWLEDGEMENTS

T. Mariella Canales was funded by the CONICYT/FONDECYT Post-Doctoral Project No. 3160248. We thank Marianela Medina and Marcelo Pájaro for their comments about the parameters used in this work.

DATA AVAILABILITY STATEMENTS

Data sharing is not applicable to this article as no new data were created or analysed in this study. Code to reproduce many of the results of the paper is available at `https://github.com/sizespectrum/plankton-anchovy`.

REFERENCES

Alheit, J. (1987). Egg cannibalism versus egg predation: their significance in anchovies. *South African Journal of Marine Science*, 5:467–470. doi:10.2989/025776187784522694.

Andersen, K. H. and Beyer, J. E. (2006). Asymptotic size determines species abundance in the marine size spectrum. *American Naturalist*, 168:54–61, doi:10.1086/504849.

Andersen, K. H., Jacobsen, N. S., Jansen, T., and Beyer, J. E. (2017). When in life does density dependence occur in fish populations? *Fish and Fisheries*, 18:656–667. doi:10.1111/faf.12195.

Anderson, J. T. (1988). A review of size dependent survival during pre-recruit stages of fishes in relation to recruitment. *Journal of Northwest Atlantic Fishery Science*, 8:55–66.

Benoît, E. and Rochet, M.-J. (2004). A continuous model of biomass size spectra governed by predation and the effects of fishing on them. *Journal of theoretical Biology*, 226:9–21.

Beverton, R. J. H. and Holt, S. J. (1957). On the dynamics of exploited fish. *Fisheries Investigations Series II Marine Fisheries of Great Britain Ministry of Agriculture, Fisheries and Food*, 19:1–533.

Blanchard, J. L., Andersen, K. H., Scott, F., Hintzen, N. T., Piet, G., and Jennings, S. (2014). Evaluating targets and trade-offs among fisheries and conservation objectives using a multispecies size spectrum model. *Journal of Applied Ecology*, 51:612–622. doi:10.1111/1365–2664.12238.

Canales, T. M., Law, R., and Blanchard, J. L. (2016). Shifts in plankton size spectra modulate growth and coexistence of anchovy and sardine in upwelling systems. *Canadian Journal of Fisheries and Aquatic Sciences*, 73:611–621. doi:/10.1139/cjfas–2015–0181.

Canales, T. M. and Leal, E. (2009). Life history parameters of anchoveta *Engraulis ringens* Jenyns, 1842, in central north Chile. *Revista de Biología Marina y Oceanografía*, 44:173–179. doi:10.4067/S0718–19572009000100017.

Castro, L., Claramunt, G., Krautz, M., Llanos-Rivera, A., and Moreno, P. (2009). Egg trait variation in anchoveta *Engraulis ringens*: a maternal response to changing environmental conditions in contrasting spawning habitats. *Marine Ecology Progress Series*, 381:237–248. doi:10.3354/meps07922.

Checkley, Jr, D. M., Asch, R. G., and Rykaczewski, R. R. (2017). Climate, anchovy, and sardine. *Annual Review of Marine Science*, 9:469–493. doi:10.1146/annurev–marine–122414–033819.

Contreras, J. E., Rodriguez-Valentino, C., Landaeta, M. F., Plaza, G., Castillo, M. I., and Alvarado-Niño, M. (2017). Growth and mortality of larval anchoveta *Engraulis ringens*, in northern Chile during winter and their relationship with coastal hydrographic conditions. *Fisheries Oceanography*, 26:603–614. doi:10.1111/fog.12219.

Cowan, Jr, J. H., Rose, K. A., and DeVries, D. R. (2000). Is density-dependent growth in young-of-the-year fishes a question of critical weight? *Reviews in Fish Biology and Fisheries*, 10:61–89. doi.org/10.1023/A:1008932401381.

Cowan, Jr, J. H., Rose, K. A., Houde, E. D., Wang, S.-B., and Young, J. (1999). Modeling effects of increased larval mortality on bay anchovy population dynamics in the mesohaline Chesapeake Bay: evidence for compensatory reserve. *Marine Ecology Progress Series*, 185:133–146. doi:10.3354/meps185133.

Cubillos, L. (1991). Estimates of monthly biomass, recruitment and fishing mortality of anchoveta (*Engraulis ringens*) off northern Chile in the period 1986–1989. *Biologia Pesquera*, 20:49–59.

Datta, S. and Blanchard, J. L. (2016). The effects of seasonal processes on size spectrum dynamics. *Canadian Journal of Fisheries and Aquatic Sciences*, 73:598–610. doi.org/10.1139/cjfas–2015–0468.

Datta, S., Delius, G. W., and Law, R. (2010). A jump-growth model for predator-prey dynamics: derivation and application to marine ecosystems. *Bulletin of Mathematical Biology*, 72:1361–1382. doi 10.1007/s11538–009–9496–5.

Di Lorenzo, E. and Ohman, M. O. (2013). A double-integration hypothesis to explain ocean ecosystem response to climate forcing. *Proceedings of the National Academy of Sciences of the United States of America*, 110 (7):2496–2499. doi.org/10.1073/pnas.1218022110.

Espinoza, P. and Bertrand, A. (2008). Revisiting Peruvian anchovy (*Engraulis ringens*) trophodynamics provides a new vision of the Humboldt Current system. *Progress in Oceanography*, 79:215–227, doi:10.1016/j.pocean.2008.10.022.

Essington, T. E., Moriarty, P. E., Froehlich, H. E., Hodgson, E. E., Koehn, L. E., Oken, K. L., Siple, M. C., and Stawitz, C. C. (2015). Fishing amplifies forage fish population collapses. *Proceedings of the National Academy of Sciences USA*, 112:6648–6652. doi:10.1073/pnas.1422020112.

Gilbert, D. J. (1997). Towards a new recruitment paradigm for fish stocks. *Canadian Journal of Fisheries and Aquatic Sciences*, 54:969–977. doi:10.1139/f96–272.

Hall, S. J., Collie, J. S., Duplisea, D. E., Jennings, S., Bravington, M., and Link, J. (2006). A length-based multispecies model for evaluating community responses to fishing. *Canadian Journal of Fisheries and Aquatic Sciences*, 63:1344–1359. doi:10.1139/f06–039.

Hartvig, M., Andersen, K. H., and Beyer, J. E. (2011). Food web framework for size-structured populations. *Journal of Theoretical Biology*, 272:113–122. doi:10.1016/j.jtbi.2010.12.006.

Hayasi, S. (1967). A note on the biology and fishery of the Japanese anchovy *Engraulis japonica* (Houttuyn). *Rep. Calif. coop. oceanic Fish. Invest. II*, 11:44–57.

Hilborn, R., Amoroso, R. O., Bogazzi, E., Jensen, O. P., Parma, A. M., Szuwalski, C., and Walters, C. J. (2017). When does fishing forage species affect their predators? *Fisheries Research*, 191:211–221. doi:10.1016/j.fishres.2017.01.008.

Houde, E. D. (1989). Comparative growth, mortality, and energetics of Maine fish larvae: temperature and implied latitudinal effects. *Fishery Bulletin*, 87:471–495.

Hsieh, C.-h., Yamauchi, A., Nakazawa, T., and Wang, W.-F. (2010). Fishing effects on age and spatial structures undermine population stability of fishes. *Aquatic Sciences*, 72:165–178. doi 10.1007/s00027–009–0122–2.

Hunter, J. R. and Kimbrell, C. A. (1980). Egg cannibalism in the northern anchovy, *Engraulis mordax*. *Fishery Bulletin*, 78:811–816.

Jordan, R. (1980). Biology of the anchoveta i: Summary of the present knowledge. *In: Proceedings of the Workshop on the Phenomenon known as El Niño*, UNESCO, Paris:249–276.

Law, R., Plank, M. J., James, A., and Blanchard, J. L. (2009). Size-spectra dynamics from stochastic predation and growth of individuals. *Ecology*, 90:802–811. doi: 10.1890/07–1900.1.

Law, R., Plank, M. J., and Kolding, J. (2012). On balanced exploitation of marine ecosystems: results from dynamic size spectra. *ICES Journal of Marine Science*, 69:602–614, doi:10.1093/icesjms/fss031.

Law, R., Plank, M. J., and Kolding, J. (2016). Balanced exploitation and coexistence of interacting, size-structured, fish species. *Fish and Fisheries*, 17:281–302. doi:10.1111/faf.12098.

Lorenzen, K. (2008). Fish population regulation beyond "stock and recruitment": the role of density-dependent growth in the recruited stock. *Bulletin of Marine Science*, 83(1):181–196.

Lorenzen, K. (2016). Toward a new paradigm for growth modeling in fisheries stock assessments: Embracing plasticity and its consequences. *Fisheries Research*, 180:4–22. dx.doi.org/10.1016/j.fishres.2016.01.006.

Lorenzen, K. and Enberg, K. (2002). Density-dependent growth as a key mechanism in the regulation of fish populations: evidence from among-population comparisons. *Proceedings of the Royal Society B: Biological Sciences*, 269:49–54. doi: 10.1098/rspb.2001.1853.

MacCall, A. D. (1980). The consequences of cannibalism in the stock-recruitment relationship of planktivorous pelagic fishes such as *Engraulis*. In Sharp, G. D., editor, *Workshop on the effects of environmental variation on the survival of larval fishes*, pages 201–220. Workshop Report 28: Intergovernmental Oceanographic Commission, UNESCO Paris.

Marañón, A. D., Cermeño, P., López-Sandoval, D. C., Rodríguez-Ramos, T., Sobrino, C., Huete-Ortega, M., Blanco, J. M., and Rodríguez, J. (2013). Unimodal size scaling of phytoplankton growth and the size dependence of nutrient uptake and use. *Ecology Letters*, 16:371–379. doi: 10.1111/ele.12052.

Murphy, G. I. (1967). Vital statistics of the Pacific sardine *Sardinops caerulea* and the population consequences. *Ecology*, 48:731–736.

O'Connell, C. P. and Raymond, L. P. (1970). The effect of food density on survival and growth of early post yolk-sac larvae of the northern anchovy (*Engraulis mordax* Girard) in the laboratory. *Journal of Experimental Marine Biology and Ecology*, 5:187–197.

Palomares, M. L., Muck, P., Mendo, J., Chuman, E., Gomez, O., and Pauly, D. (1987). Growth of the Peruvian anchoveta *Engraulis ringens*, 1953-1982. In Pauly, D. and Tsukayama, I., editors, *The Peruvian anchoveta and its upwelling ecosystem: three decades of changes*, pages 117–141. ICLARM Studies and Reviews 15.

Peebles, E. B., Hall, J. R., and Tolley, S. G. (1996). Egg production by the bay anchovy *Anchoa mitchilli* in relation to adult and larval prey fields. *Marine Ecology Progress Series*, 131:61–73.

Plank, M. J. and Law, R. (2012). Ecological drivers of stability and instability in marine ecosystems. *Theoretical Ecology*, 5:465–480. doi:10.1007/s12080–011–0137–x.

Pájaro, M. (1998). El canibalism como mecanismo regulador denso-dependiente de mortalidad natural en la anchoíta (*Engraulis anchoita*). Su relación con las estrategias reproductivas de la especies. Tesis Doctoral. *Universidad Nacional de Mar del Plata, Argentina.*

Pájaro, M. and Ciechomski, J. (1996). Canibalismo de la anchoita adulta (*Engraulis anchoita*) sobre postlarvas, en un area de cria de la especies. *Frente Marino*, 16:131–139.

Pájaro, M., Curelovich, J., and Macchi, G. J. (2007). Egg cannibalism in the northern population of the Argentine anchovy, *Engraulis anchoita* (Clupeidae). *Fisheries Research*, 83:253–262, doi:10.1016/j.fishres.2006.09.014.

Ricker, W. E. (1954). Stock and recruitment. *Journal of the Fisheries Research Board of Canada*, 11:559–623.

Ricker, W. E. and Foerster, R. E. (1948). Computation of fish production. *Bulletin of the Bingham Oceanographic Collection*, 11:173–211.

Rose, K. A., Cowan, Jr, J. H., Winemiller, K. O., Myers, R. A., and Hilborn, R. (2001). Compensatory density dependence in fish populations: importance, controversy, understanding and prognosis. *Fish and Fisheries*, 2:293–327. doi:10.1046/j.1467–2960.2001.00056.x.

Rossberg, A. G., Houle, J. E., and Hyder, K. (2013). Stock-recruitment relations controlled by feeding interactions alone. *Canadian Journal of Fisheries and Aquatic Sciences*, 70:1447–1455. doi:10.1139/cjfas–2012–0531.

Rothschild, B. J. (2000). "Fish stocks and recruitment": the past thirty years. *ICES Journal of Marine Science*, 57:191–201. doi:10.1006/jmsc.2000.0645.

Salvacetti, R., Field, D., Gutiérrez, D., Baumgartner, T., Ferreira, V., Ortlieb, L., Sifeddine, A., Grados, D., and Bertrand, A. (2018). Multifarious anchovy and sardine regimes in the Humboldt Current System during the last 150 years. *Global Change Biology*, 24:1055–1068. doi:10.1111/gcb.13991.

Schwartzlose, R. A., Alheit, J., Bakun, A., Baumgartner, T. R., Cloete, R., Crawford, R. J. M., Fletcher, W. J., Green-Ruiz, Y., Hagen, E., Kawasaki, T., Lluch-Belda, D., Lluch-Cota, S. E., MacCall, A. D., Matsuura, Y., Nevárez-Martínez, M. O., Parrish, R. H., Roy, C., Serra, R., Shust, K. V., Ward, M. N., and Zuzunaga, J. Z. (1999). Worldwide large-scale fluctuations of sardine and anchovy populations. *South African Journal of Marine Science*, 21:289–347. doi:/10.2989/025776199784125962.

Scott, F., Blanchard, J. L., and Andersen, K. H. (2014). MIZER: an R package for multispecies, trait-based and community size spectrum ecological modelling. *Methods in Ecology and Evolution*, 5:1121–1125. doi: 10.1111/2041–210X.12256.

Silvert, W. and Platt, T. (1978). Energy flux in the pelagic ecosystem: a time-dependent equation. *Limnology and Oceanography*, 23:813–816.

Skjæraasen, J. E., Nash, R. D. M., Korsbrekke, K., Fonn, M., Nilsen, T., Kennedy, J., Nedreaas, K. H., Thorsen, A., Witthames, P. R., Geffen, A. J., Høie, H., and Kjesbu, O. S. (2012). Frequent skipped spawning in the world's largest cod population. *Proceedings of the National Academy of Sciences USA*, 109:8995–8999. doi:10.1073/pnas.1200223109.

Sogard, S. M. (1997). Size-selective mortality in the juvenile stage of teleost fishes: a review. *Bulletin of Marine Science*, 60:1129–1157.

Stige, L. C., Rogers, L. A., Neuheimer, A. B., Hunsicker, M. E., Yaragina, N. A., Ottersen, G., Ciannelli, L., Langangen, Ø., and Durant, J. M. (2019). Density- and size-dependent mortality in fish early life stages. *Fish and Fisheries*, 20:962–976. doi: 10.1111/faf.12391.

Svedäng, H. and Hornborg, S. (2015). Waiting for a flourishing Baltic cod (*Gadus morhua*) fishery that never comes: old truths and new perspectives. *ICES Journal of Marine Science*, 72:2197–2208. doi:10.1093/icesjms/fsv112.

Szuwalski, C. S., Vert-Pre, K. A., Punt, A. E., Branch, T. A., and Hilborn, R. (2015). Examining common assumptions about recruitment: a meta-analysis of recruitment dynamics for worldwide marine fisheries. *Fish and Fisheries*, 16:633–648. doi:10.1111/faf.12083.

Takasuka, A., Yoneda, M., and Oozeki, Y. (2019a). Density dependence in total egg production per spawner for marine fish. *Fish and Fisheries*, 20:125–137. doi:10.1111/faf.12327.

Takasuka, A., Yoneda, M., and Oozeki, Y. (2019b). Disentangling density-dependent effects on egg production and survival from egg to recruitment in fish. *Fish and Fisheries*, 20:870–887. doi:10.1111/faf.12381.

Turchin, P. (1995). Population regulation: old arguments and a new synthesis. In Cappuccino, N. and Price, P. W., editors, *Population Dynamics: New Approaches and Synthesis*, chapter 2, pages 19–39. Academic Press, San Diego, California.

Valdés-Szeinfeld, E. (1991). Cannibalism and intraguild predation in clupeoids. *Marine Ecology Progress Series*, 79:17–26. doi:10.3354/meps079017.

van Gemert, R. and Andersen, K. H. (2018). Challenges to fisheries advice and management due to stock recovery. *ICES Journal of Marine Science*, 75(6):1864–1870. doi:10.1093/icesjms/fsy084.

APPENDICES

A Mathematical model

Because body mass of size spectra can span many orders of magnitude, it helps to make a transformation from body mass to a dimensionless logarithm of body mass, $x = \ln(w/w_0)$, where w is body mass and w_0 is an arbitrary body mass of, say, 1 g. We adopt this transformation throughout.

A.1 Fish population dynamics

We work with a state variable for a single species of fish, $u(x,t)dx = \phi(w,t)dw$, with dimensions L^{-3}, which corresponds to the density of individuals with log body mass in a small range $[x, x+dx]$ at time t. This is referred to as a size spectrum, and is a function of body size x, changing shape over the course of time t.

The dynamics can be written in terms of the following partial differential equation describing the flux in density $u(x,t)$ (Law et al., 2016):

$$\frac{\partial u}{\partial t} = \underbrace{-\frac{\partial}{\partial x}\left[\epsilon g u\right]}_{\text{(a)}} - \underbrace{du}_{\text{(b)}} - \underbrace{\mu u}_{\text{(c)}} + \underbrace{\epsilon_R R \frac{b}{w_0 e^x}}_{\text{(d)}} + \underbrace{\frac{1}{2}\frac{\partial}{\partial x}\left[e^{-x}\frac{\partial}{\partial x}\left[\epsilon G u\right]\right]}_{\text{(e)}}, \tag{A.1}$$

where function arguments x and t have been suppressed for clarity. This equation is based on a second-order approximation to a jump-growth model, which itself is a systematic expansion of a master equation from a stochastic predator-prey process in which organisms grow and die through eating one another (Datta et al., 2010).

In Eq. (A.1), term (a) describes the flux in density due to somatic growth, where $\epsilon(x)$ is the proportion of incoming food mass allocated to somatic growth, and $g(x,t)$ is a mass-specific growth rate. Term (b) describes cannibalism, where $d(x,t)$ is the per-capita death rate from this source. Term (c) deals with intrinsic deaths, including both larval and background mortality, at per capita rate $\mu(x)$. Term (d) describes the total birth rate, obtained by transforming the total rate $R(t)$ at which reproductive mass is created into a distribution at which eggs of different sizes are created, through an egg-size distribution function $b(x)$; this rate is weighted by an efficiency ϵ_R with which the reproductive mass is turned into female eggs. Term (e) is a second-order diffusion process that allows growth trajectories to spread out as the fish grow, where $G(x,t)$ is a second-order growth term. The motivation for and description of the functions are described below.

Note that the lower and upper bounds of body size in Eq. (A.1) are determined by features of reproduction. Specifically, the lower boundary is set by the function $b(x)$, assumed here to be a Dirac delta function that renews the population at a

single egg size $w_0 e^{x_0}$. The upper boundary is set by the maximum size $w_0 e^{x_\infty}$ to which fish grow, which is typically very close to the size at which all incoming food is allocated to reproduction.

Feeding kernel. At the heart of the model there is a function describing the preference of consumers for the size of prey items, relative to their own size, often called a feeding kernel. This has usually been thought of as a Gaussian function on the scale of log body mass, centred on a preferred predator-prey mass ratio for a consumer species, around which feeding declines to zero (Benoît and Rochet, 2004; Andersen and Beyer, 2006; Datta et al., 2010). However, planktivores filter water through gill rakers, more passively removing prey items, and may be better described by an unselective function. We therefore use a box kernel which is unselective on the log scale of body mass over a chosen size range relative to the consumer:

$$s(x'-x) = \begin{cases} \dfrac{1}{6\sigma} & x-\beta-3\sigma < x < x'-\beta+3\sigma \\ 0 & \text{otherwise} \end{cases}. \tag{A.2}$$

normalised by $\frac{1}{6\sigma}$ to integrate to 1. The function is given in this form so that the parameters β and σ can be interpreted in the same way as those in a Gaussian feeding kernel, β being the centre of the kernel, and 6σ being its width, beyond which particles are not filtered.

Cannibalism. The feeding kernel is needed for the per capita death rate $d(x)$ from cannibalism at body size x:

$$d(x) = \int A(w_0 e^{x'})^\alpha s(x'-x)\theta u(x')dx'. \tag{A.3}$$

This equation is the convolution of the feeding kernel and cannibal densities over cannibal sizes x', to get the overall effect of consumers on the death rate at size x. The expression $A(w_0 e^{x'})^\alpha$ introduces a scaling of the feeding rate with cannibal size (parameter α). The parameter A sets the dimensions of the death rate to 1/time.

Mass-specific growth rate. Closely related to Eq. (A.3) is the growth rate of the fish at body size x, as they themselves feed on smaller particles, including both plankton and smaller anchovy. This is given here as a mass-specific growth rate $g(x)$ at size x:

$$g(x) = AK(w_0 e^x)^\alpha e^{-x} \int e^{x'} s(x-x') \Big(u_p(x') + \theta u(x') \Big) dx'. \tag{A.4}$$

The convolution in this case is over food items (x'), both small fish $u(x')$ and plankton $u_p(x)$ (see Eq. (A.11)), and is converted to mass by the term $w_0 e^{x'}$. Parameters A and α are as in Eq. (A.3). The extra parameter θ allows cannibalism to be switched on or off. K is the food conversion efficiency, i.e. the efficiency with

which prey biomass is converted into consumer biomass; for the sake of simplicity, this is as far as the model goes into metabolic processes.

Larval mortality rate. We assume the extra risks of mortality at the larval stage are represented by a per-capita larval mortality rate $\mu_l(x)$ of body size x:

$$\mu_l(x) = \mu_{\underline{l}} \frac{e^{\rho_l(x_{\bar{l}}-x)}}{1+e^{\rho_l(x_{\bar{l}}-x)}}. \tag{A.5}$$

This is a reverse-sigmoid function that starts large on eggs, and falls to zero as the fish get big enough to leave the vulnerable stage. The function contains three parameters: (1) the magnitude of the extra mortality rate $\mu_{\underline{l}}$, as the larval stage begins, (2) the body size $x_{\bar{l}}$ at which fish are growing out of the vulnerable larval stage, and (3) the range of body size ρ_l over which this escape takes place.

Background mortality rate. This accounts for all intrinsic mortality other than the larval component. In keeping with earlier work (Hartvig et al., 2011), this per-capita mortality rate $\mu_b(x)$ scales to decrease with body size x for the most part. However, as the fish get near to their asymptotic mass, it starts to increase again, taking the form:

$$\mu_b(x) = \begin{cases} \mu_0\, e^{-\rho_b(x-x_0)} & x_0 \le x \le x_s \\ \mu_b(x_s)\, e^{\rho_s(x-x_s)} & x_s < x \le x_\infty \end{cases}. \tag{A.6}$$

Here μ_0 is the background death rate at birth, $\mu_b(x_s)$ is the background death rate at size x_s where the death rate starts to increase, and ρ_b, ρ_s are the exponents for the sensitivity of death to body size.

Total intrinsic mortality rate. Summing the per-capita rates of larval and background mortality gives the total per-capita intrinsic death rate:

$$\mu(x) = \mu_l(x) + \mu_b(x), \tag{A.7}$$

i.e. the term $\mu(x)$ in Eq. (A.1).

Reproduction. The function $1-\epsilon(x)$ describes the proportion of incoming food allocated to reproduction, and uses an expression suggested by Hartvig et al. (2011) and Law et al. (2012)

$$1-\epsilon(x) = \begin{cases} \overbrace{[1+\exp(-\rho_m(x-x_m))]^{-1}}^{(a)} \overbrace{\exp(\rho_\infty(x-x_\infty))}^{(b)} & x < x_\infty \\ 1 & \text{otherwise.} \end{cases} \tag{A.8}$$

Part (a) deals with maturation, where x_m is the body size at which 50 % of the fish are mature, and ρ_m defines the body-size range over which fish are maturing. Part (b) describes allocation to reproduction once maturity is reached. The maximum body size x_∞ is typically very close the size at which all incoming mass is allocated to reproduction and no further somatic growth is possible, the approach to x_∞ being

scaled by a parameter ρ_∞. The total rate R at which reproductive mass density is created is then given by:

$$R = \int (1 - \epsilon(x)) g(x) u(x) w_0 e^x dx. \tag{A.9}$$

This takes the mass-specific rate at which reproductive mass is created at size x, converts it to the total rate at size x by multiplying by density and mass at size x, and lastly integrates over all sizes x. The total mass rate is converted into a rate of egg production, using an egg distribution function $b(x)$. Dividing by the size of eggs at x, then converts the mass density rate into the rate at which eggs appear at this size, $\epsilon_R \, R \, b(x) \, / \, (w_0 e^x)$, where the term $\epsilon_R < 1$ allows some inefficiency in converting the reproductive mass into eggs. For simplicity, we take $b(x)$ to be a Dirac delta function at x_0, so all eggs appear at the single size $w_0 e^{x_0}$.

Diffusion. The second-order diffusion term allows growth trajectories of fish to spread as they get older—without this all fish born at the same time would have identical trajectories of growth (Datta et al., 2010). The diffusion term contains a function

$$G(x) = AK^2 (w_0 e^x)^\alpha e^{-x} \int e^{2x'} s(x - x') \Big(u_p(x') + \theta u(x') \Big) dx', \tag{A.10}$$

for the most part resembling the mass-specific growth rate in Eq. (A.4) where the terms are defined.

A.2 Plankton dynamics

We work with a state variable for the plankton $u_p(x,t)dx = \phi_p(w,t)dw$, corresponding to the density of cells with log cell mass in a small range $[x, x + dx)$ at time t. The rate of change of plankton density $u_p(x)$ at size x, is written as:

$$\frac{\partial u_p}{\partial t} = \underbrace{r u_p \big(1 - u_p/a\big)}_{\text{(a)}} + \underbrace{i}_{\text{(b)}} - \underbrace{d u_p}_{\text{(c)}}. \tag{A.11}$$

Here the intrinsic rate of increase $r(x)$, the carrying capacity $a(x)$, and the immigration rate $i(x)$ scale with body mass w $(= w_0 e^x)$ as:

$$\begin{aligned} r(x) &= r_0 (w_0 e^x)^{\rho - 1} \\ a(x) &= a_0 (1000 w_0 e^x)^{-\lambda + 1} \\ i(x) &= i_0 (1000 w_0 e^x)^{-\lambda + 1} \end{aligned} \tag{A.12}$$

The function $r(x)$ takes into account a scaling of cell division rate with cell size with an exponent $\rho - 1$, over a range of cell sizes (Marañón et al., 2013); the parameter r_0 sets the overall rate. The function $a(x)$ is the carrying capacity in the absence

of immigration and planktivory; it ensures that, in the absence of planktivory, plankton would settle to an equilibrium size spectrum that scales with cell size with an exponent $-\lambda + 1$; the parameter a_0 locates the function that describes the equilibrium. The function $i(x)$ scales with body size in the same way as the carrying capacity. The function $d(x)$ is the per-capita death rate from planktivory by anchovy. This is similar to cannibalism in anchovy, Eq. (A.3):

$$d_p(x) = \int A(w_0 e^{x'})^\alpha s(x' - x) u(x') dx', \tag{A.13}$$

except that the planktivory by anchovy is always present.

B Partitioning mortality within cohorts

The key equation for following a cohort over time is Eq. (2.3) in the text. The numerical solution of this describes cohort growth as the cohort ages, i.e. the average size of individuals in the cohort at each age τ, given birth at time t_0, $x_c(\tau; t_0)$; for shorthand, we write this as $x_c(\tau)$. Components of mortality in the cohort at age τ correspond to components of mortality in the size-spectrum model at $t = t_0 + \tau$ as follows:

$$\begin{aligned} d(x_c(\tau)) &= d(x, t) \\ \mu_l(x_c(\tau)) &= \mu_l(x, t) \\ \mu_b(x_c(\tau)) &= \mu_b(x, t), \end{aligned} \tag{B.1}$$

where the death rates $d(x, t)$, $\mu_l(x, t)$ and $\mu_b(x, t)$ are defined in Eqs (A.3), (A.5) and (A.6) respectively. In other words, the component death rates in the cohort are extracted directly from the numerical integration of the size-spectrum model. The proportion S_T in the cohort surviving to age T is then:

$$\begin{aligned} S_T &= e^{\int_0^T d(x_c(\tau)) + \mu_l(x_c(\tau)) + \mu_b(x_c(\tau))\ d\tau} \\ &= S_{T,d}\ S_{T,\mu_l}\ S_{T,\mu_b}. \end{aligned} \tag{B.2}$$

In this way, the components of survivorship to age T from birth at time t_0 are partitioned into survival from cannibalism $S_{T,d}$, survival from larval death S_{T,μ_l}, and survival from background death S_{T,μ_b}.

Importantly, the cohort interacts with all other cohorts that are present in the population during its life. For instance, a cohort born before t_0 that suffered greater fixed larval mortality resulting in a lower density as an adult would contribute less to cannibalism in the cohort born at time t_0. This is because the earlier, depleted cohort makes a smaller contribution to $d(x)$ (Eq. (A.3)), and hence to $d(x_c)$.

C Parameter values

This appendix gives values of parameters as used for simulations of the mathematical model in Appendix A. Parameter values for anchovy and plankton are in Table 1 and 2 respectively. The parameter w_0 is set at 1 g.

Lower and upper bounds for the anchovy size spectrum were set by an egg mass at 0.0003 g, and a maximum body mass at 66.5 g (Castro et al., 2009; Cubillos, 1991).

We used a 'box'-shaped feeding kernel (Eq. (A.2)) to reflect the relatively unselective filter-feeding of planktivores. Lower and upper limits of the kernel were set relative to the size of the feeding anchovy at 1/30000, and 1/100 respectively. This means, for instance, that an individual at egg size would filter particles in the range from 10^{-8} g to 3×10^{-6} g. An individual at 30 g would consume particles in the range from 10^{-3} g to 3×10^{-1} g; this upper limit is consistent with copepods and euphausiids forming part of the diet of large anchovy (Espinoza and Bertrand, 2008). Anchovy always fed on plankton ($\theta_p = 1$, Eq. (A.4), (A.10)), and cannibalism was switched off ($\theta = 0$), or on ($\theta = 1$), as required. A value of the feeding-rate parameter $A = 750$ m^3 yr^{-1} g$^{-\alpha}$ was chosen so that anchovy would grow from egg mass to 10 g in approximately 1 yr (Canales and Leal, 2009), when the deterministic system with cannibalism was near to steady state. The food conversion efficiency was set at $K = 0.1$.

Following the literature (Contreras et al., 2017), a large larval mortality rate was used at egg size, the exact value $\mu_{\underline{l}} = 21$ yr^{-1} (Eq. (A.5)) being chosen to be close to the smallest value that would stabilise the deterministic dynamics. We assumed the fish would be leaving the larval stage at around 100 times the egg weight (around 0.03 g), after which this component of mortality became negligible. This body mass was reached at an age of about 90 d when the deterministic system with cannibalism was near to steady state (Contreras et al., 2017). On the basis that most mortality would be associated with the larval state early in life, background mortality was taken to be a small proportion of it (Eq. (A.6)) $\mu_0 = 1$ yr^{-1}, falling with increasing body size up to 0.5 g, at which size it started to increase again.

For reproduction, anchovy was assumed to mature around 10 g (Canales and Leal, 2009). Reproductive efficiency was set at 0.1, lower than the value that would apply just on the basis of a standard sex ratio of 0.5, on the grounds that some extra costs are likely in gonad development and reproductive behaviour.

Table 1: Anchovy parameters.

parameter	value	interpretation
$w_0 e^{x_0}$	0.0003 g	egg mass
$w_0 e^{x_\infty}$	66.5 g	maximum body mass
β	7.46	centre of feeding kernel
σ	0.951	measure of the width of feeding kernel
A	750 $\mathrm{m}^3\ \mathrm{yr}^{-1}\ \mathrm{g}^{-\alpha}$	feeding rate constant
α	0.85	search-rate scaling exponent
K	0.1	ecological conversion efficiency
$\mu_{\underline{l}}$	21 yr^{-1}	larval death rate at egg size
$w_0 e^{x_{\bar{l}}}$	0.03 g	size around which larval death $\to 0$
ρ_l	5	exponent scaling size range as larval death $\to 0$
μ_0	1 yr^{-1}	background death rate at birth
$w_0 e^{x_s}$	0.5 g	body mass at minimum background death rate
ρ_b	0.25	exponent scaling falling death rate with size
ρ_s	1	exponent scaling increasing death rate with size
$w_0 e^{x_m}$	10 g	body mass at 50 % maturity
ρ_m	15	exponent scaling size range of maturation
ρ_∞	0.2	exponent scaling approach to $x_{i,\infty}$
ϵ_R	0.1	reproductive efficiency

Table 2: Plankton parameters.

parameter	value	interpretation
$w_0 e^{x_{p,0}}$	10^{-10} g	minimum cell mass
$w_0 e^{x_{p,\infty}}$	10^{-1} g	maximum body mass
r_0	10 $\mathrm{g}^{1-\rho}\ \mathrm{yr}^{-1}$	sets intrinsic rate to 10 yr^{-1} at 1 g
a_0	100 $\mathrm{m}^{-3}\ \mathrm{g}^{\lambda-1}$	sets 'equilibrium' density to 100 m^{-3} at 1 mg
i_0	100 $\mathrm{m}^{-3}\ \mathrm{g}^{\lambda-1}\ \mathrm{yr}^{-1}$	sets immigration rate 100 $\mathrm{m}^{-3}\ \mathrm{yr}^{-1}$ at 1 mg
ρ	0.85	scales intrinsic rate with respect to x
λ	2	scales slope of 'isolated' size spectrum

The term 'equilibrium' refers to an isolated plankton assemblage at cell size 1 mg. The term 'isolated' refers to a plankton spectrum lacking immigration and predation.